Biochemical and Biophysical Research Communications 666 (2023) 68–75

Contents lists available at ScienceDirect

Biochemical and Biophysical Research Communications

journal homepage: www.elsevier.com/locate/ybbrc

Curcumin tautomerization in the mechanism of pentameric amyloid-β42 oligomers disassembly

Atsuya Matsui [a], Jean-Pierre Bellier [b, **], Daiki Hayashi [a], Takafumi Ishibe [c], Yoshiaki Nakamura [c], Hiroyasu Taguchi [d], Nobuyasu Naruse [a, *], Yutaka Mera [a]

[a] Department of Fundamental Bioscience, Shiga University of Medical Science, Otsu, 520-2192, Japan
[b] Neurology Department, Brigham and Women's Hospital, Boston, MA, 02115, USA
[c] Graduate School of Engineering Science, Osaka University, 1-3 Machikaneyama-Cho, Toyonaka, Osaka, 560-8531, Japan
[d] Kyoto Women's University, Kitahiyoshi-cho, Higashiyama-ku, Kyoto, 605-8501, Japan

ARTICLE INFO

Article history:
Received 6 April 2023
Accepted 22 April 2023
Available online 3 May 2023

Keywords:
Amyloid-β
Oligomers
Curcumin
Atomic force microscopy
Tautomerism

ABSTRACT

Alzheimer's disease is a neurologic disorder characterized by the accumulation of extracellular deposits of amyloid-β (Aβ) fibrils in the brain of patients. The key etiologic agent in Alzheimer's disease is not known; however oligomeric Aβ appears detrimental to neuronal functions and increases Aβ fibrils deposition. Previous research has shown that curcumin, a phenolic pigment of turmeric, has an effect on Aβ assemblies, although the mechanism remains unclear. In this study, we demonstrate that curcumin disassembles pentameric oligomers made from synthetic Aβ42 peptides (pentameric oAβ42), using atomic force microscopy imaging followed by Gaussian analysis. Since curcumin shows keto-enol structural isomerism (tautomerism), the effect of keto-enol tautomerism on its disassembly was investigated. We have found that curcumin derivatives capable of keto-enol tautomerization also disassemble pentameric oAβ42, while, a curcumin derivative incapable of tautomerization did not affect the integrity of pentameric oAβ42. These experimental findings indicate that keto-enol tautomerism plays an essential role in the disassembly. We propose a mechanism for oAβ42 disassembly by curcumin based on molecular dynamics calculations of the tautomerism. When curcumin and its derivatives bind to the hydrophobic regions of oAβ42, the keto-form changes predominantly to the enol-form; this transition is associated with structural (twisting, planarization and rigidification) and potential energy changes that give curcumin enough force to act as a torsion molecular-spring that eventually disassembles pentameric oAβ42. This proposed mechanism sheds new light on keto-enol tautomerism as a relevant chemical feature for designing such novel therapeutic drugs that target protein aggregation.

1. Introduction

Alzheimer's disease (AD) is a progressive neurologic disorder that accounts for 60–80% of all dementia [1]. AD is characterized by the accumulation of amyloid plaques in the brains of patients [2,3]. The proteolytic sequential cleavage of the transmembrane amyloid protein precursor by β- and γ-secretase results in the production of Aβ peptides of 36–43 amino acids in size [4]. Aβ peptides are hydrophobic and, therefore, have a strong tendency to bind with various hydrophobic molecules, including other Aβ peptides, and on cell membranes, such as the synaptic termination of neurons [5–7]. Among Aβ peptides, the 42 amino acid form (Aβ42) is a major component of amyloid plaques that are generally considered to cause synaptic loss and neurodegeneration in AD [8]. Aβ42 oligomers (e.g. oAβ42s) have been described to exert neurotoxic effects, increase Aβ fibrillation, and promote the hyperphosphorylation of the tau protein, another key pathological feature of AD progression in neurons [8–13].

Studying the oAβ42s formation pathway and thermodynamic equilibrium is challenging because oAβ42s are transient protein complexes with a metastable structural conformation [9]. Many methods were applied to assess oAβ42 formation with mixed success. Fluorescent assays based on probing beta-sheet in Aβ42 fibrils, e.g., with thioflavin-T, showed limitations when used to

* Corresponding author.
** Corresponding author.
E-mail addresses: jbellier1@bwh.harvard.edu (J.-P. Bellier), naruse@belle.shiga-med.ac.jp (N. Naruse).

https://doi.org/10.1016/j.bbrc.2023.04.076

assess the formation of oAβ42s. Cryo-electron microscopy, a powerful tool to study the structural biology of fibrils, did not reach the required structural resolution of oligomers [14]. Atomic force microscopy (AFM) has been used to characterize oligomeric assemblies from synthetic Aβ42 peptides [15–17], and Gaussian fitting analysis of height histograms from AFM topographic images were used successfully to identify and quantify oAβ42s [18–20].

Recently, we established an experimental design where the test compound was added to a solution of pentameric oAβ42 that was prepared from synthetic Aβ42 monomers. The homogeneous preparation of pentameric oAβ42 was first reported by Ahmed et al. [7], and successfully reproduced in several laboratories and the formation of pentameric oAβ42 was confirmed using different methods [7,20,21]. The advantage of such a preparation resides in its homogeneous composition that facilitates monitoring the effect of a drug on it, as any change in oAβ42 composition would directly reflect changes in pentameric oAβ42 integrity. By using AFM imaging, we were able to assess changes in oAβ42s composition after ethanol treatment which was followed by Gaussian fitting analysis. We observed that ethanol concentrations higher than 1.4 M (8.3%) resulted in the disassembly of pentameric oAβ42 [20]. Incubation with lower concentrations had no effect and could be used for studying the lipophilic/hydrophobic aspects of compounds that need to be dissolved in organic solvents [22].

Curcumin, the yellow pigment found in the rhizome of *Curcuma longa* turmeric, is a natural polyene-phenol with a 1,3-dicarbonyl group that exhibits keto-enol structural isomerism (tautomerism). Curcumin exists in the diketo-form in water and in the enol-form in organic solvents (Fig. 2) [23–25]. Curcumin has been shown to bind or inhibit the formation of amyloid-β assemblies and plaques [26–29]. Curcumin and its derivatives were reported to bind Aβ aggregates including insoluble fibrils and soluble oligomers [30–32]. The anti-amyloid mechanism of this curcumin interaction remains unclear, though it was suggested that various aspects of curcumin, such as its antioxidant, anti-inflammatory, and metal-chelating properties, could be involved [33]. In a specific study, the effect of curcumin on Aβ-oligomers was reported but the investigation rather focused on the hydrolyzates of curcumin on such oligomers [34]. Only a few computational approaches addressed the mechanism of Aβ-oligomer destabilization by curcumin from a structural perspective though no mechanism has been proposed yet [35–37].

Herein, we report studies of the effect of curcumin on an essentially homogeneous preparation of the pentameric oAβ42 using AFM imaging followed by Gaussian analysis. Next, we investigated the role of curcumin tautomerism using curcumin derivatives with or without the ability of tautomerization. Finally, we deduced a possible mechanism of disassembly based on the tautomeric properties of curcumin using molecular dynamics analysis.

2. Materials and methods

2.1. Materials

Amyloid-β1-42 (human, trifluoroacetate) (Aβ42) was purchased from Peptide Institute (Osaka, Japan); purity and identity were confirmed by the manufacturer using UV/mass spectrometry, high-performance liquid chromatography and amino acid analysis. Low-protein binding microtubes and tips were used. Unless otherwise

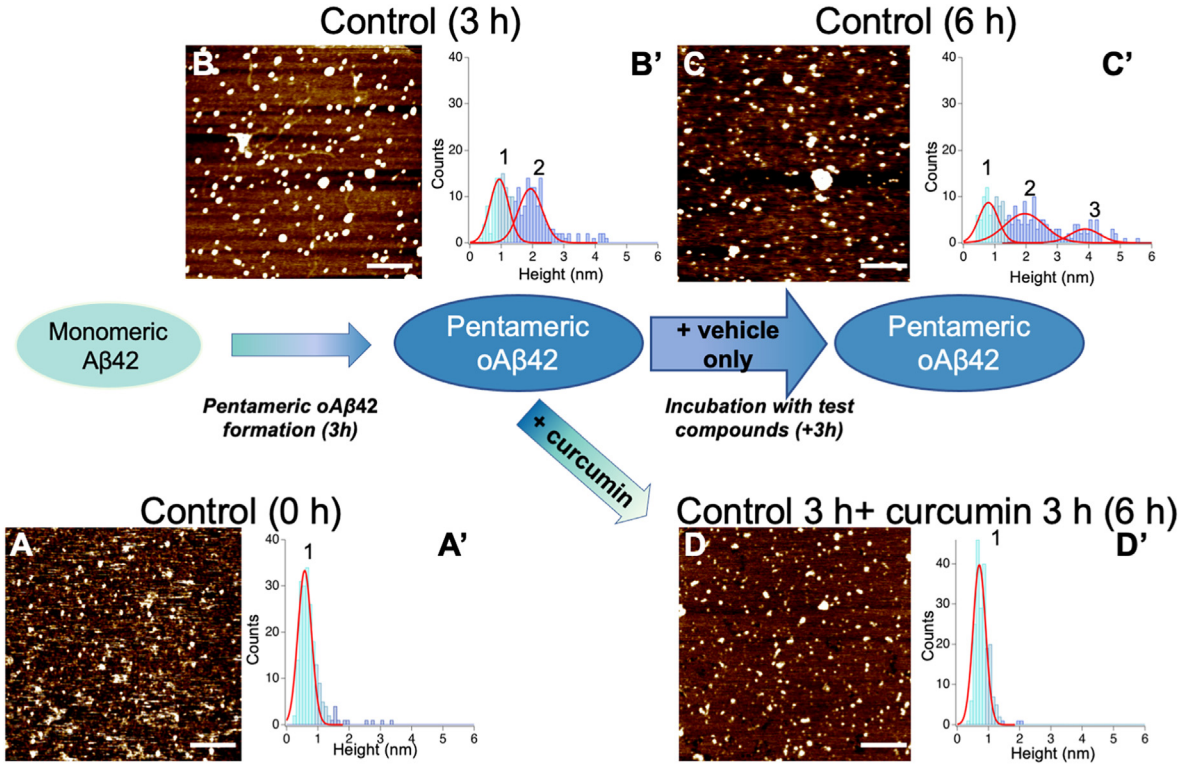

Fig. 1. Typical topographic AFM images (A–D) and the contrast height histograms (A′-D′) from monomeric and oAβ42s. A freshly prepared made solution of monomeric Aβ42 peptide (A and A′) solution was incubated for 3-hrs at 4 °C to form pentameric oAβ42 (B and B′). This latter solution was incubated with the control alone (C and C′) or with 120 μM curcumin dissolved in the control (D and D′). Gaussian fitting curves are shown in red on histograms (A′-D′). The scale bar of AFM images is 200 nm, and the contrast represents the height size through color scale (black to white: 0 nm to 1.0 nm height, except in A and D where the scale is from 0 nm to 0.5 nm). For histograms, heights less than 0.89 nm are shown in light blue (monomers), heights from 0.89 to 1.5 nm in blue, and heights over 1.5 nm in purple (pentamers) (see Supplementary Fig. 1). The number of counted contrasts in each aliquot is more than 200. (For interpretation of the references to color in this figure legend, the reader is referred to the Web version of this article.)

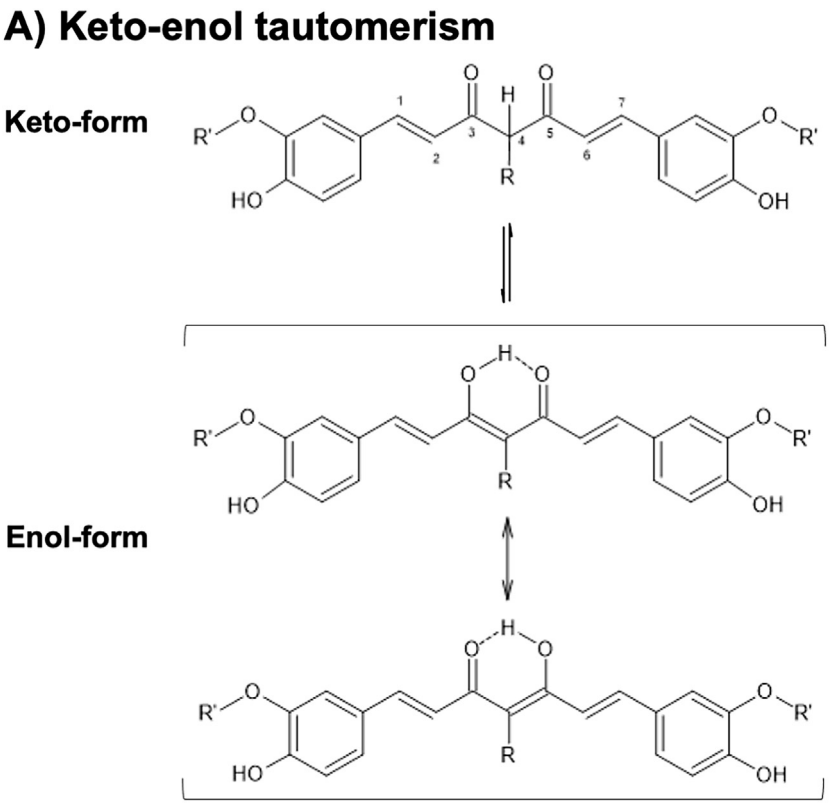

Compounds	R	R’
Curcumin	H	CH_3
compound 1	CH_3	CF_3
compound 2	$CH_2CH_2COOCH_3$	CF_3

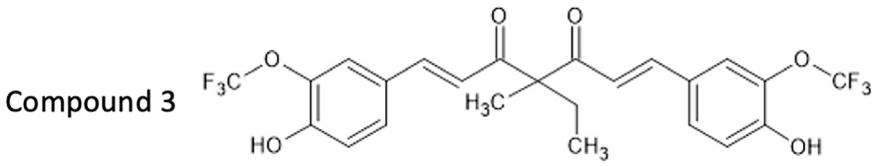

Fig. 2. Tautomerism of curcumins A) Curcumins: the double harpoons between the keto-form and the enol-form represent the equilibrium between the two forms. The enol-form of curcumin is represented as a resonance hybrid of two canonical forms connected with a double-headed arrow. B) compound 3: The two hydrogen atoms at the C-4 position are replaced by methyl- and ethyl-group, and this compound is not capable of tautomerization to an enol form.

indicated, all the reagents were purchased from Fujifilm (Osaka, Japan).

2.2. Sample preparation

As introduced in our previous study, oligomers of Aβ42 were prepared by the method of Ahmed et al. with slight modifications as described here [7,20,21]. Monomeric Aβ42 was prepared by dissolving the contents of one vial of synthetic peptides in 170 μL of hexafluoro-2-propanol (HFIP), followed by 20 min of ultra-sonication and quick removal of HFIP by vacuum lyophilization. A 0.12 mM solution of the monomer was prepared by dissolving the lyophilized preparation into 510 μL of cooled (4 °C) buffer solution (3.5% of 0.1 M NaOH in 0.05 M phosphate buffer solution (pH 7.4) containing 0.05 M NaCl). The resulting solution was incubated for 3-hrs in dark at 4 °C to promote the formation of pentameric oAβ42. After the incubation, a 10 μL solution of 2.1 mM curcumin solution freshly dissolved in pure ethanol (Nacalai Tesque Kyoto, Japan) was added to one tube (The final concentration of curcumin is 120 μM and ethanol is 5.6% in the tube). And also 10 μL of pure ethanol was added to another tube as the control. For experiments using curcumin derivatives [38] (compound 1 [39], compound 2 [30] and compound 3 [31]), 10 μL of a 2.1 mM solution was added to another tube (final concentration: 0.12 mM compounds 1, 2, and 3 in 5.6%

ethanol, respectively). The tubes were further incubated for 3-hrs at 4 °C. For AFM analysis, 10 μL aliquots from each tube were taken at the indicated time intervals and immediately processed; the remaining samples were quickly frozen in liquid nitrogen, lyophilized using vacuum drying, and stored at −80 °C until required.

2.3. AFM observation and analysis

Aliquots of the above-prepared solutions were diluted 200-times with cold (4 °C) Milli-Q water, and 8 μL of this solution were dropped onto a freshly cleaved mica disc (V-1 Grade 9.5 nm φ × 0.15 nm, Alliance Biosystems Co., Ltd, Osaka, Japan), then dried quickly in cool dark space. Dried mica samples were washed with ethanol and Milli-Q water for 20 s each, then quickly dried under vacuum. This step was performed in order to improve AFM observation by reducing artifacts on the mica surface due to different hydration landscapes resulting from curcumin, potassium carbonate crystals, and other crystals from the buffer solution [40,41]. Topographic images of the preparation were obtained using an AFM Innova system (Bruker, USA) operating in the air under ambient humidity and room temperature. The system was equipped with a silicon cantilever (RTESP-150, Bruker, USA) showing a spring constant of 5 N/m (nominal value) and a tip radius of 8–12 nm. Measurements were performed in tapping mode, with a resonant frequency of about 110 kHz and a scanning rate of 0.7 Hz (1 line per sec.). AFM topographic images (1 × 1 μm and 512 × 512 pixels) were acquired using the software NanoDrive (v8.02, Bruker, USA). Cross-sectional profiles of the images were analyzed with the Gwyddion software (v.2.56, Czech Metrology Institute, Czech Republic) after the elimination of the scanning noise and tip curvature artifact by Gaussian fitting using Igor Pro 9 (HULINKS Inc., Japan) [16,42]. The height histograms derived from AFM topographic images were also analyzed by Gaussian fitting to identify oAβ42s as shown in Supplementary Fig. 1. The height values of spherical Aβ42s appearing in circular contrasts of AFM data were measured from cross-sectional analysis; as it is more accurate than the direct determination of the width from AFM measurements, which are not necessarily absolute values because of convolution between the AFM tip and particle radius [43,44].

2.4. Molecular dynamics

MD was performed using MOE software (Molecular Operating Environment v2020.0901, Chemical Computing Group, Montreal, Canada). The molecules were energy minimized after protonation using the Amber10 forcefield parameters, and a 10/12 Å cuton/cutoff was used for both van der Waals and electrostatic interactions. Next, the solvation of curcumin tautomers was simulated in water containing NaCl 0.1 M for keto-form and DMSO for enol-form. Then, a conformational search for the most thermodynamically favorable conformation was performed using a low-ModeMD algorithm [45].

3. Results and discussion

3.1. Disassembly of Aβ pentamers by curcumin

We studied the effect of curcumin on pentameric oAβ42 using our recently established experimental design that combines AFM, and statistical analysis [20]. Briefly, a freshly prepared solution of monomeric synthetic Aβ42 was incubated for 3-hrs under carefully controlled parameters (temperature, pH, salt, and initial monomer concentration) to promote the preferential formation of pentameric oAβ42, then curcumin (or vehicle only) was added, and changes in pentameric oAβ42 composition were assessed using AFM followed by height histogram with Gaussian curve analysis (Fig. 1, see Supplementary Figs. 1 and 2) [18,20]. AFM measurements confirmed that oAβ42s were homogeneously pentameric assemblies with heights of about 2 nm (Fig. 1B). Aβ oligomerization is expected to be in equilibrium [46,47], and AFM height histograms with Gaussian curve can statistically estimate the abundance of Aβ assemblies (Figs. 1 and 3 and Supplementary Figs. 1 and 2). Topographic AFM images of the solution containing pentameric oAβ42 showed roughly circular contrasts of various sizes and shapes (Fig. 1A–D). Small-sized contrasts were observed in solutions made of freshly dissolved monomeric Aβ42 (Fig. 1A). The height histogram analysis of these small-sized contrasts showed a single Gaussian peak at 0.58 ± 0.31 nm (Fig. 1A, peak 1), which fits the expected average height of the Aβ42 monomer [20,46,48,49]. When the same solution was incubated for 3-hrs at 4 °C to form pentameric oAβ42, topographic AFM images showed larger-sized contrasts (Fig. 1B) and two Gaussian peaks at 0.94 ± 0.41 nm and 1.9 ± 0.41 nm (Fig. 1B', peak 1 and 2, respectively). The peak at 1.9 nm is consistent with the height of pentameric oAβ42 [7,15,20,48]. The peak around 0.9 nm is interpreted as a mixture of dimer, trimer, and tetramers (small-sized oligomers). These results indicated that the solution was essentially composed of successfully assembled Aβ42s. After that, the solution was divided into two aliquots; one was incubated for continuing 3-hrs at 4 °C for Aβ42 control solution (5.6% ethanol final concentration) (Fig. 1C), and another was incubated for continuing 3-hrs at 4 °C with 120 μM curcumin in control (Fig. 1D). This concentration of ethanol has no effect on oAβ42s [20]. When the control solution incubated for 6-hrs was assessed using Gaussian analysis of height distribution, three peaks were observed. Spherical contrasts with large heights obviously increased between 0 and 6 h, which indicated that oligomerization was progressing over the time. The first two were observed at 0.79 ± 0.43 nm and 1.9 ± 0.88 nm (Fig. 1C', peak 1 and 2, respectively), similar to those observed after the initial 3-hrs incubation (Fig. 1B'). The third peak detected at 3.9 ± 0.66 nm was similar to what was previously described after 6-hrs of continuous incubation [7] and interpreted as the stack of two pentamers (double-layered pentamer) [7,20,34,50]. This observation indicated that the control did not significantly impact the integrity of pentameric oAβ42. In contrast, the solution of pentameric oAβ42 incubated with 120 μM curcumin showed dramatic differences. The size of the contrasts was smaller (Fig. 1D), and the histogram analysis only showed a single peak at 0.70 ± 0.31 nm (Fig. 1D', peak 1). This peak was most reasonably interpreted as the mixture of monomeric Aβ42 and oAβ42s of smaller complexity (i.e., dimer, trimer, and tetramer) than the initial solution containing essentially of pentameric oAβ42 (Fig. 1B', peak 2: 1.9 ± 0.41 nm). It is noteworthy to mention that the left-ward shift of the histogram peak indicating the disassembly of pentamers into small-sized Aβ units was observed as rapidly as within 30 min after the addition of curcumin to pentameric oAβ42 (see Supplementary Fig. 2ii). Incorporation of curcumin in pentameric oAβ42 occurs quickly and a reasonable amount of the pentamer was disassembled after the addition of curcumin. These results indicated that curcumin disassembled pentameric oAβ42 into a mixture of small-sized oligomers and Aβ42 monomers.

3.2. Dissolution and hydrolysis of curcumin in buffer

As far as we know, only one paper investigated the effect of curcumin on the Aβ oligomers [34] by using AFM and NMR to assess

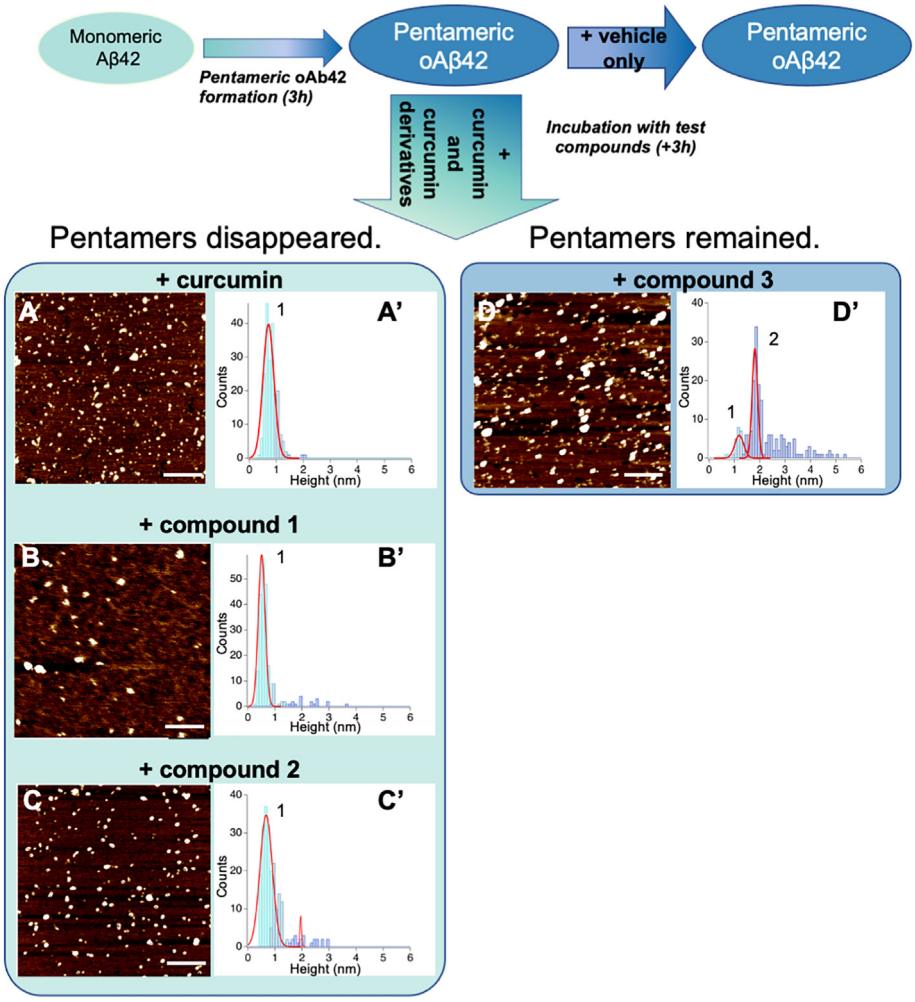

Fig. 3. Typical AFM topographic images (A–D) and histogram distribution of contrast height (A′-D′) of solutions containing pentameric oAβ42 incubated for 3-hrs at 4 °C with the curcumin derivatives (A: curcumin, B: compound 1, C: compound 2, and D: compound 3). The red curves of peaks were derived from Gaussian fitting in the same way as Fig. 1. Fig. 3A'-C′ had monomeric peaks around 0.6–0.7 nm including smaller amounts of small-sized oligomers (<pentamers). The sharp peak 2 at 1.8 nm in Fig. 3D' corresponded to the pentameric oAβ42. Incidentally, this peak position was also present in Fig. 3C', albeit slightly. Histograms are colored in light blue (monomer), blue (dimer-tetramer), and purple (pentamer), similar to Fig. 1. The number of counted contrasts in each aliquot is more than 200. The scale bar of AFM images is 200 nm, and the contrast represents the height size through the color scale (black to white: 0 nm to 1 nm height). Table 1: the peak height values of Gaussian curves (mean ± standard deviation). For reference, the table shows the heights of monomeric and pentameric peptides determined from the control solutions in Fig. 1 (cf. 1). (For interpretation of the references to color in this figure legend, the reader is referred to the Web version of this article.)

Aβ oligomers after the addition of "curcumin". Because of the low solubility of curcumin in aqueous buffer at neutral pH, the authors used 100 mM sodium hydroxide solution to dissolve curcumin. Curcumin is unstable in alkaline solution, and degrades to vanillin, ferulic acid, feruloyl methane, and *trans*-6-(4′-hydroxy-3′-methoxyphenyl)-2,4-dioxo-5-hexenal and 100 mM sodium hydroxide is a strong enough base to hydrolyze curcumin in a short period of time [51]. In this context, it is quite possible that the majority of their AFM and NMR data would reveal the effect of the hydrolyzates of curcumin on Aβ oligomers rather than curcumin itself. Herein, we used ethanol as solvent for curcumin. In our previous report, we determined the limited concentration of ethanol that does not affect Aβ (ethanol 8.3%) and established a method of adding curcumin to oligomeric Aβ42 incubation after preparing the amphipathic ethanolic solution of curcumin, taking advantage of the fact that curcumin exists in both hydrophilic and hydrophobic neutral solvents due to tautomerism [25,51].

3.3. *Tautomerization of curcumin*

Curcumin is a compound with the peculiarity to exhibit keto-enol tautomerism. It is well known that such compounds tend to ketonize in an aqueous solution and to enolize in hydrophobic solvents [23,24]. In an aqueous solution, curcumin is mostly in the keto-form but is thermodynamically unfavored in ethanol because of its hydrophobicity, and then curcumin would try to evade this by partitioning into a hydrophobic environment or by binding to other hydrophobic molecules; in both cases, it would enolize. Ahmed et al. and Tran et al. [7,50] proposed that the conformational stability of disk-shaped oAβ42 pentamers/decamers is the result of the hydrophobic C-terminus is concealed from the aqueous solvent, facing either the mica surface for pentamers or facing another pentamer hydrophobic surface to form decamers. The same phenomenon should occur when curcumin encounters pentameric oAβ42, it would bind to the hydrophobic region of pentameric oAβ42 and then would enolize. In this context, we raise the question of whether the enolization associated with tautomerization

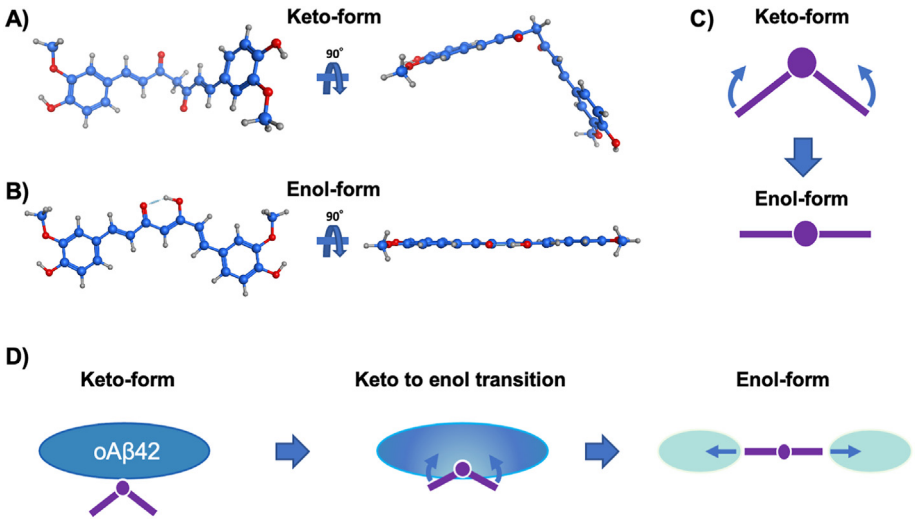

Fig. 4. Most favorable thermodynamic conformation for curcumin tautomeric forms. A) Curcumin keto-form conformation; search was simulated in water containing 0.1 M NaCl. The side view is on the right. B) Curcumin enol-form conformation; search was simulated in DMSO. Curcumin enol-form has a coplanar conformation. The side view is on the right. C) Schematic representation of the structural change during keto to enol tautomerization, torsional action, planarization, and rigidification of curcumin which could be compared to the action of a torsion spring. D) Schematic representation of the proposed mechanism of pentameric oAβ42 (large blue ellipse) disassembly through tautomerization of curcumin (purple). Curcumin keto-form binds to the hydrophobic region of oAβ42. The hydrophobic environment would promote the keto-to-enol transition with torsional action, planarization and rigidification of curcumin enol-form that may apply enough forces to disassemble pentameric oAβ42 into lower complexity oligomers or monomers (small green ellipse). This action could be compared to the action of a "torsion molecular-spring" (arrows). (For interpretation of the references to color in this figure legend, the reader is referred to the Web version of this article.)

could be the driver of the mechanism leading to the disassembly of pentameric oAβ42.

3.4. Effect of the tautomerism on pentameric oAβ42

To test the above hypothesis, we investigated the effect of curcumin derivatives (i.e., compound 1 [38,39], compound 2 [30,38], and compound 3 [31,38]) towards pentameric oAβ42. Compounds 1 and 2 are mono-alkylated derivatives at the C-4 position of curcumin (Fig. 2). They are subject to keto-enol tautomerism similar to that of curcumin, because of the presence of a hydrogen atom at C-4. Compound 3, however, is a di-alkylated derivative (Fig. 2) at the C-4 position in which similar tautomerization *cannot* take place, and the compound retains its keto-form in any solvent [31,38]. When solutions containing pentameric oAβ42 were incubated for 3-hrs at 4 °C with compound 1 under similar conditions to those for curcumin, topographic AFM imaging was very similar to those for curcumin. The histogram analysis showed a major peak at the height of 0.60 ± 0.17 nm (Fig. 3B) which corresponds to monomers (0.58 ± 0.31 nm). The slight difference between 0.58 nm and 0.60 nm could be attributed to the mixture of monomers and small amounts of small-sized oligomers. Larger oligomers (around 2 nm) were detected but the amounts were small and almost negligible (Supplementary Fig. 1). Compound 2 gave similar results to those for compound 1 (Fig. 3C). The height of the peak at 0.67 ± 0.32 nm was similar to that for curcumin but spread further than for compound 1 (0.60 ± 0.17 nm). The height of the peak is probably the result from the ratio of a large amount of monomer and some small-sized oligomers. However, Compound 3 gave a result totally different from those of the other curcumin derivatives (Fig. 3D). No peaks were observed at around 0.7 nm in the AFM histogram which should appear if the pentameric oAβ was disassembled. Instead, the histogram analysis showed the presence of various sizes of oAβ42 (from 1 to 6 nm) and a major peak at the height of 1.8 ± 0.14 nm which corresponds to pentameric oAβ42. The effect of curcumin derivatives which are not capable of keto-enol tautomerization is interesting and under investigation. Gaussian fitting curves and colored histograms indicated nicely whether incubated pentamers were changed to different aggregate sizes by the addition of curcumin derivatives. Considering the experimental data mentioned above, it would be reasonable to conclude that curcumins capable of keto-enol tautomerism can disassemble pentameric oAβ42, but the disassembly does not take place with the curcumin derivatives which cannot enolize.

3.5. Molecular Dynamics of tautomerism with torsion, flexibility, and rigidity

Next, we investigated how enolization associated with tautomerization promotes the disassembly of pentameric oAβ42. We used molecular dynamics (MD) analysis to search for the most favorable thermodynamic conformation for curcumin keto-form and enol-form. The conformations resulting from this analysis are shown in Fig. 4. The most stable conformation for the curcumin keto-form in water-NaCl (Fig. 4A) showed that the two carbonyl groups at C3 and C5 position were in a trans conformation with the carbonyl oxygen atoms as far apart as possible; this conformation is similar to those reported previously [25]. The most stable conformation for the curcumin enol-form was easier to envisage because, during the enolization, the intramolecular hydrogen bonding in the

Table 1
Peak location values of the red Gaussian curves in height distributions.

oAβ+compd	peak 1	peak 2
A' (+curcumin)	0.70 ± 0.31	–
B' (+ compound 1)	0.60 ± 0.17	–
C' (+ compound 2)	0.67 ± 0.32	1.9 ± 0.04
D' (+compound 3)	1.2 ± 0.25	1.8 ± 0.14
cf. 1 Control solution	Peak location	
Monomer Aβ42	0.58 ± 0.31	
pentameric oAβ42	1.9 ± 0.41	

(mean ± standard deviation).
All values in nm.

Table 2
Calculated potential energies for the curcumin keto- and enol-forms, together with their relative energies.

	Keto -form in water-NaCl	Enol-form in DMSO	*ΔE*
Total potential energy	−5.32	0.14	5.46
Bond strench potential energy	1.24	1.5	0.26
Angle bend potential energy	10.43	11.05	0.62
Out-of-plane potential energy	0.15	0	−0.15
Torsion potential energy	14.26	8.17	−6.09
Van der Waals component of the potential energy	11.83	16.9	5.07
Electrostatic component of potential energy	−43.24	−37.49	5.75

All values in kcal/mol.

center of the molecule (Fig. 2A) stabilizes the enolic form and causes the delocalization of electrons toward the peripheral ring; this will first tend to repulse both rings and result in a conformation that should be more planar than the keto-form. Concomitantly the rings should adopt a co-planar conformation. MD search of the thermodynamically favorable conformations for curcumin enol-form in DMSO illustrates this situation perfectly (Fig. 4B). These simulations indicated that the enolization would stiffen the structure of curcumin into a relatively planar conformation; the flexible keto-form is transformed into the rigid enol-form. The calculated potential energies for the curcumin keto- and enol-forms are shown in Table 2, together with their relative energies in their most thermodynamically favorable conformation. Most noticeable ∂E changes were observed for the torsion potential energy, which 'won' in stability, while energy absorption was observed for electrostatic and van der Waals components. Taken together, MD analysis of the thermodynamically favorable conformation and potential energy calculations indicated that the tautomerization of curcumin from keto-form to enol-form is associated with important structural (torsional, rigidification, and planarization) and potential energy change, which might give curcumin enough structural force to eventually act as a "torsion molecular-spring" (Fig. 4C). When curcumin binds to pentameric oAβ42, and if the binding energy (van der Waals and other forces) to form the pentamer is lower than the energy difference between the keto- and the enol-form then tautomerization may result in the application of a strong structural force onto the hydrophobic region of pentameric oAβ42, ultimately resulting in its disassembly (Fig. 4D).

In Aβ42, which is a relatively small peptide, the contact area between peptide oligomers formed from it is limited and the forces of mutual attraction are weak enough to cause the oligomers to be disassembled by the keto-enol tautomerization. In the case of larger peptides/proteins, as the size of the protein increase, the contact area increases too, and therefore a greater attractive force is expected for disassembly. At some point, the attractive force would be higher than the energy released during the keto-to-enol transition, and disassembly of the protein complex by curcumin will not be possible. However, many compounds exhibit 1,3-dicarbonyl groups, such as the one involved in curcumin tautomerism. They probably have different energy releases during keto-to-enol transition, or it could be increased by chemical modification. Therefore, the mechanism proposed here may open a new avenue in designing such drugs able to disassemble peptides/protein complexes.

Declaration of competing interest

The authors declare the following financial interests/personal relationships which may be considered as potential competing interests: Nobuyasu Naruse reports financial support was provided by Grant-in-Aid for Scientific Research (C) from the Japan Society for the Promotion of Science (KAKENHI) Grant Number 19K05207. Nobuyasu Naruse reports a relationship with the Japan Society for the Promotion of Science that includes: funding grants. Nobuyasu Naruse has patent pending to Nobuyasu Naruse. The authors declare no competing interest.

Acknowledgment

We are grateful to Prof. Ikuo Tooyama and Prof. Yoshio Furusho of the Shiga University of Medical Science, and Dr. Wilfred L. F. Armarego of the Australian National University for critically reading the manuscript. This work was partly supported by a Grant-in-Aid for Scientific Research (C) from the Japan Society for the Promotion of Science KAKENHI Grant Number 19K05207.

Appendix A. Supplementary data

Supplementary data to this article can be found online at https://doi.org/10.1016/j.bbrc.2023.04.076.

References

[1] 2022 Alzheimer's disease facts and figures, Alzheimer's Dementia 18 (2022) 700–789, https://doi.org/10.1002/alz.12638.
[2] R.A. Stelzmann, H. Norman Schnitzlein, F. Reed Murtagh, über eine eigenartige erkankung der hirnrinde, Clin. Anat. 8 (1995) 429–431, https://doi.org/10.1002/ca.980080612.
[3] J. Therriault, E.R. Zimmer, A.L. Benedet, T.A. Pascoal, S. Gauthier, P. Rosa-Neto, Staging of Alzheimer's disease: past, present, and future perspectives, Trends Mol. Med. 28 (2022) 726–741, https://doi.org/10.1016/j.molmed.2022.05.008.
[4] C. Haass, C. Kaether, G. Thinakaran, S. Sisodia, Trafficking and proteolytic processing of APP, Cold Spring Harb Perspect Med 2 (2012), https://doi.org/10.1101/cshperspect.a006270 a006270–a006270.
[5] L. Vugmeyster, M.A. Clark, I.B. Falconer, D. Ostrovsky, D. Gantz, W. Qiang, G.L. Hoatson, Flexibility and solvation of amyloid-β hydrophobic core, J. Biol. Chem. 291 (2016) 18484–18495, https://doi.org/10.1074/jbc.M116.740530.
[6] T.L. Williams, L.C. Serpell, Membrane and surface interactions of Alzheimer's Aβ peptide - insights into the mechanism of cytotoxicity, FEBS J. 278 (2011) 3905–3917, https://doi.org/10.1111/j.1742-4658.2011.08228.x.
[7] M. Ahmed, J. Davis, D. Aucoin, T. Sato, S. Ahuja, S. Aimoto, J.I. Elliott, W.E. Van Nostrand, S.O. Smith, Structural conversion of neurotoxic amyloid-β 1-42 oligomers to fibrils, Nat. Struct. Mol. Biol. 17 (2010) 561–567, https://doi.org/10.1038/nsmb.1799.
[8] M.P. Lambert, A.K. Barlow, B.A. Chromy, C. Edwards, R. Freed, M. Liosatos, T.E. Morgan, I. Rozovsky, B. Trommer, K.L. Viola, P. Wals, C. Zhang, C.E. Finch, G.A. Krafft, W.L. Klein, Diffusible, nonfibrillar ligands derived from Aβ1-42 are potent central nervous system neurotoxins, Proc. Natl. Acad. Sci. U. S. A. 95 (1998) 6448–6453, https://doi.org/10.1073/pnas.95.11.6448.
[9] E.N. Cline, M.A. Bicca, K.L. Viola, W.L. Klein, The amyloid-β oligomer hypothesis: beginning of the third decade, J. Alzheim. Dis. 64 (2018) S567–S610, https://doi.org/10.3233/JAD-179941.
[10] W.B. Stine, K.N. Dahlgren, G.A. Krafft, M.J. LaDu, In vitro characterization of conditions for amyloid-β peptide oligomerization and fibrillogenesis, J. Biol. Chem. 278 (2003) 11612–11622, https://doi.org/10.1074/jbc.M210207200.
[11] S. Li, M. Jin, T. Koeglsperger, N.E. Shepardson, G.M. Shankar, D.J. Selkoe, Soluble a β oligomers inhibit long-term potentiation through a mechanism involving excessive activation of extrasynaptic NR2B-containing NMDA receptors, J. Neurosci. 31 (2011) 6627–6638, https://doi.org/10.1523/JNEUROSCI.0203-11.2011.
[12] S. Oddo, A. Caccamo, L. Tran, M.P. Lambert, C.G. Glabe, W.L. Klein, F.M. LaFerla, Temporal profile of amyloid-β (Aβ) oligomerization in an in vivo model of Alzheimer disease: a link between Aβ and tau pathology, J. Biol. Chem. 281 (2006) 1599–1604, https://doi.org/10.1074/jbc.M507892200.

[13] D.M. Walsh, I. Klyubin, J.v. Fadeeva, W.K. Cullen, R. Anwyl, M.S. Wolfe, M.J. Rowan, D.J. Selkoe, Naturally secreted oligomers of amyloid β protein potently inhibit hippocampal long-term potentiation in vivo, Nature 416 (2002) 535–539, https://doi.org/10.1038/416535a.
[14] J.-P. Renaud, A. Chari, C. Ciferri, W. Liu, H.-W. Rémigy, H. Stark, C. Wiesmann, Cryo-EM in drug discovery: achievements, limitations and prospects, Nat. Rev. Drug Discov. 17 (2018) 471–492, https://doi.org/10.1038/nrd.2018.77.
[15] I.A. Mastrangelo, M. Ahmed, T. Sato, W. Liu, C. Wang, P. Hough, S.O. Smith, High-resolution atomic force microscopy of soluble Aβ42 oligomers, J. Mol. Biol. 358 (2006) 106–119, https://doi.org/10.1016/j.jmb.2006.01.042.
[16] F. Simone Ruggeri, J. Habchi, A. Cerreta, G. Dietler, AFM-based single molecule techniques: unraveling the amyloid pathogenic species, Curr. Pharmaceut. Des. 22 (2016) 3950–3970, https://doi.org/10.2174/1381612822666160518141911.
[17] S. Banerjee, M. Hashemi, Z. Lv, S. Maity, J.C. Rochet, Y.L. Lyubchenko, A novel pathway for amyloids self-assembly in aggregates at nanomolar concentration mediated by the interaction with surfaces, Sci. Rep. 7 (2017) 1–11, https://doi.org/10.1038/srep45592.
[18] Y.C. Lin, H. Komatsu, J. Ma, P.H. Axelsen, Z. Fakhraai, Quantitative analysis of amyloid polymorphism using height histograms to correct for tip convolution effects in atomic force microscopy imaging, RSC Adv. 6 (2016) 114286–114295, https://doi.org/10.1039/C6RA24031C.
[19] J. Marek, E. Demjénová, Z. Tomori, J. Janáček, I. Zolotová, F. Valle, M. Favre, G. Dietler, Interactive measurement and characterization of DNA molecules by analysis of AFM images, Cytometry 63 (2005) 87–93, https://doi.org/10.1002/cyto.a.20105.
[20] A. Matsui, J.-P. Bellier, T. Kanai, H. Satooka, A. Nakanishi, T. Terada, T. Ishibe, Y. Nakamura, H. Taguchi, N. Naruse, Y. Mera, The effect of ethanol on disassembly of amyloid-β1-42 pentamer revealed by atomic force microscopy and gel electrophoresis, Int. J. Mol. Sci. 23 (2022) 889, https://doi.org/10.3390/ijms23020889.
[21] N. Elizabeth Pryor, M.A. Moss, C.N. Hestekin, Unraveling the early events of amyloid-ß protein (Aß) aggregation: techniques for the determination of Aβ aggregate size, Int. J. Mol. Sci. 13 (2012) 3038–3072, https://doi.org/10.3390/ijms13033038.
[22] K. Pagano, S. Tomaselli, H. Molinari, L. Ragona, Natural compounds as inhibitors of Aβ peptide aggregation: chemical requirements and molecular mechanisms, Front. Neurosci. 14 (2020), https://doi.org/10.3389/fnins.2020.619667.
[23] A.G. Cook, P.M. Feltman, Determination of solvent effects on keto—enol equilibria of 1,3-dicarbonyl compounds using NMR, J. Chem. Educ. 84 (2007) 1827, https://doi.org/10.1021/ed084p1827.
[24] O. Kazakova, N. Lipkovska, V. Barvinchenko, Keto-enol tautomerism of curcumin in the preparation of nanobiocomposites with fumed silica, Spectrochim. Acta Mol. Biomol. Spectrosc. 277 (2022), 121287, https://doi.org/10.1016/J.SAA.2022.121287.
[25] Y. Manolova, V. Deneva, L. Antonov, E. Drakalska, D. Momekova, N. Lambov, The effect of the water on the curcumin tautomerism: a quantitative approach, Spectrochim. Acta Mol. Biomol. Spectrosc. 132 (2014) 815–820, https://doi.org/10.1016/j.saa.2014.05.096.
[26] K. Ono, K. Hasegawa, H. Naiki, M. Yamada, Curcumin has potent anti-amyloidogenic effects for Alzheimer's β-amyloid fibrils in vitro, J. Neurosci. Res. 75 (2004) 742–750, https://doi.org/10.1002/jnr.20025.
[27] F. Yang, G.P. Lim, A.N. Begum, O.J. Ubeda, M.R. Simmons, S.S. Ambegaokar, P. Chen, R. Kayed, C.G. Glabe, S.A. Frautschy, G.M. Cole, Curcumin inhibits formation of amyloid β oligomers and fibrils, binds plaques, and reduces amyloid in vivo, J. Biol. Chem. 280 (2005) 5892–5901, https://doi.org/10.1074/jbc.M404751200.
[28] M. Garcia-Alloza, L.A. Borrelli, A. Rozkalne, B.T. Hyman, B.J. Bacskai, Curcumin labels amyloid pathology in vivo, disrupts existing plaques, and partially restores distorted neurites in an Alzheimer mouse model, J. Neurochem. 102 (2007) 1095–1104, https://doi.org/10.1111/j.1471-4159.2007.04613.x.
[29] M. Necula, R. Kayed, S. Milton, C.G. Glabe, Small molecule inhibitors of aggregation indicate that amyloid β oligomerization and fibrillization pathways are independent and distinct, J. Biol. Chem. 282 (2007) 10311–10324, https://doi.org/10.1074/jbc.M608207200.
[30] D. Yanagisawa, H. Taguchi, A. Yamamoto, N. Shirai, K. Hirao, I. Tooyama, Curcuminoid binds to amyloid-β1-42 oligomer and fibril, J. Alzheim. Dis. 24 (2011) 33–42, https://doi.org/10.3233/JAD-2011-102100.
[31] D. Yanagisawa, T. Kato, H. Taguchi, N. Shirai, K. Hirao, T. Sogabe, T. Tomiyama, K. Gamo, Y. Hirahara, M. Kitada, I. Tooyama, Keto form of curcumin derivatives strongly binds to Aβ oligomers but not fibrils, Biomaterials 270 (2021), 120686, https://doi.org/10.1016/j.biomaterials.2021.120686.
[32] A.A. Reinke, J.E. Gestwicki, Structure-activity relationships of amyloid beta-aggregation inhibitors based on curcumin: influence of linker length and flexibility, Chem. Biol. Drug Des. 70 (2007) 206–215, https://doi.org/10.1111/j.1747-0285.2007.00557.x.
[33] M. Tang, C. Taghibiglou, The mechanisms of action of curcumin in Alzheimer's disease, J. Alzheim. Dis. 58 (2017) 1003–1016, https://doi.org/10.3233/JAD-170188.
[34] Z. Fu, D. Aucoin, M. Ahmed, M. Ziliox, W.E. Van Nostrand, S.O. Smith, Capping of Aβ42 oligomers by small molecule inhibitors, Biochemistry 53 (2014) 7893–7903, https://doi.org/10.1021/bi500910b.
[35] P.P.N. Rao, T. Mohamed, K. Teckwani, G. Tin, Curcumin binding to beta amyloid: a computational study, Chem. Biol. Drug Des. 86 (2015) 813–820, https://doi.org/10.1111/cbdd.12552.
[36] I. Doytchinova, M. Atanasova, E. Salamanova, S. Ivanov, I. Dimitrov, Curcumin inhibits the primary nucleation of amyloid-beta peptide: a molecular dynamics study, Biomolecules 10 (2020) 1323, https://doi.org/10.3390/biom10091323.
[37] O. Zoltán, P. László, K. Éva, V. Béla, A "keto-enol" plaque buster mechanism to diminish Alzheimer's β-Amyloid burden, Biochem. Biophys. Res. Commun. 532 (2020) 82–87, https://doi.org/10.1016/j.bbrc.2020.07.086.
[38] H. Taguchi, D. Yanagisawa, S. Morikawa, K. Hirao, N. Shirai, I. Tooyama, Synthesis and tautomerism of curcumin derivatives and related compounds, Aust. J. Chem. 68 (2015) 224–229, https://doi.org/10.1071/CH14464.
[39] D. Yanagisawa, N. Shirai, T. Amatsubo, H. Taguchi, K. Hirao, M. Urushitani, S. Morikawa, T. Inubushi, M. Kato, F. Kato, K. Morino, H. Kimura, I. Nakano, C. Yoshida, T. Okada, M. Sano, Y. Wada, K. nosuke Wada, A. Yamamoto, I. Tooyama, Relationship between the tautomeric structures of curcumin derivatives and their Aβ-binding activities in the context of therapies for Alzheimer's disease, Biomaterials 31 (2010) 4179–4185, https://doi.org/10.1016/j.biomaterials.2010.01.142.
[40] F. Ostendorf, C. Schmitz, S. Hirth, A. Kühnle, J.J. Kolodziej, M. Reichling, Evidence for potassium carbonate crystallites on air-cleaved mica surfaces, Langmuir 25 (2009) 10764–10767, https://doi.org/10.1021/la901311k.
[41] W. Trewby, D. Livesey, K. Voïtchovsky, Buffering agents modify the hydration landscape at charged interfaces, Soft Matter 12 (2016) 2642–2651, https://doi.org/10.1039/c5sm02445e.
[42] Y. Gan, Atomic and subnanometer resolution in ambient conditions by atomic force microscopy, Surf. Sci. Rep. 64 (2009) 99–121, https://doi.org/10.1016/j.surfrep.2008.12.001.
[43] J.D. Harper, S.S. Wong, C.M. Lieber, P.T. Lansbury, Observation of metastable Aβ amyloid protofibrils by atomic force microscopy, Chem. Biol. 4 (1997) 119–125, https://doi.org/10.1016/S1074-5521(97)90255-6.
[44] P.N. Nirmalraj, J. List, S. Battacharya, G. Howe, L. Xu, D. Thompson, M. Mayer, Complete aggregation pathway of amyloid β (1-40) and (1-42) resolved on an atomically clean interface, Sci. Adv. 6 (2020), https://doi.org/10.1126/sciadv.aaz6014.
[45] P. Labute, LowModeMD - implicit low-mode velocity filtering applied to conformational search of macrocycles and protein loops, J. Chem. Inf. Model. 50 (2010) 792–800, https://doi.org/10.1021/ci900508k.
[46] K. Ono, M.M. Condron, D.B. Teplow, Structure-neurotoxicity relationships of amyloid β-protein oligomers, Proc. Natl. Acad. Sci. U. S. A. 106 (2009) 14745–14750, https://doi.org/10.1073/pnas.0905127106.
[47] S. Nag, B. Sarkar, A. Bandyopadhyay, B. Sahoo, V.K.A. Sreenivasan, M. Kombrabail, C. Muralidharan, S. Maiti, Nature of the amyloid-β monomer and the monomer-oligomer equilibrium, J. Biol. Chem. 286 (2011) 13827–13833, https://doi.org/10.1074/jbc.M110.199885.
[48] S. De, D.C. Wirthensohn, P. Flagmeier, C. Hughes, F.A. Aprile, F.S. Ruggeri, D.R. Whiten, D. Emin, Z. Xia, J.A. Varela, P. Sormanni, F. Kundel, T.P.J. Knowles, C.M. Dobson, C. Bryant, M. Vendruscolo, D. Klenerman, Different soluble aggregates of Aβ42 can give rise to cellular toxicity through different mechanisms, Nat. Commun. 10 (2019) 1541, https://doi.org/10.1038/s41467-019-09477-3.
[49] D. Losic, L.L. Martin, A. Mechler, M.I. Aguilar, D.H. Small, High resolution scanning tunnelling microscopy of the β-amyloid protein (Aβ1-40) of Alzheimer's disease suggests a novel mechanism of oligomer assembly, J. Struct. Biol. 155 (2006) 104–110, https://doi.org/10.1016/j.jsb.2006.02.013.
[50] L. Tran, N. Basdevant, C. Prévost, T. Ha-Duong, Structure of ring-shaped Aβ42 oligomers determined by conformational selection, Sci. Rep. 6 (2016), 21429, https://doi.org/10.1038/srep21429.
[51] S. D, Y.S. Kumavat, P. Chaudhari, P. Borole, K. Mishra, P. Duvvuri Shenghani, Degradation studies of curcumin, Int. J. Pharmaceut. Sci. Rev. Res. 3 (2013) 50–55. http://www.ijprr.com/File_Folder/50-55.pdf.